International Journal of Thin Films Science and Technology

http://dx.doi.org/10.18576/ijtfst/110301

Study of the Optical Properties of Zno Nano-structure at Different Ti Content

E. A. Badawi[1,*], H. Ibrahim[1], M. R. Ebied[1], M. Abdel-Rahman[1], H. Khallaf[1], M. A. Abdel Rahman[1], E. E. Assem[2] and A. Ashour[1,2].

[1]Physics Department, Faculty of Science, Minia University, 61519, Minia, Egypt
[2]Physics Department, Faculty of Science, Islamic University, Medina, Kingdom of Saudi Arabia

Received: 13 May. 2022, Revised: 2 Jul. 2022, Accepted: 21 Jul. 2022.
Published online: 1 Sep. 2022.

Abstract: Zinc oxide (ZnO) and TZO samples having different Ti content were synthesized from doping to composite by Citrate sol-gel method (dissolving and react with citric acid) characterized according to their optical properties. The UV - vis characterization exhibiting good optical properties**.** The results show there are one absorption edge at pure and low Ti doping but at higher Ti% another edge appeared and slightly shifted around 400 nm**.** The maximum absorption nearly at 350 nm, and the band gap energy of Ti-doped ZnO increase from 3**.**16 to 3**.**20 eV achieving a blue-shift. A red shift from 3**.**07 to 3**.**19 eV in the visible range which has a very important application, this improves the optical properties of ZnO and gives an indication how to tune its band gap (increase or decrease by doping or composition)**.**

Keywords : Optical properties**,** Ti-Doped ZnO, ZnO/TiO_2 nano-composites, ZnO nanostructure.

1. Introduction

The optical properties of a semiconductor are connected with both intrinsic and extrinsic effects**.** Intrinsic optical transitions take place between the electrons in the conduction band and holes in the valence band, including excitonic effects due to the Coulomb interaction**.** Excitons are classified into free and bound excitons**.** In high-quality samples with low impurity concentrations, the free exciton can also exhibit excited states, in addition to their ground-state transitions**.** Extrinsic properties are related to dopants or defects, which usually create discrete electronic states in the band gap, and therefore influence both optical-absorption and emission processes [1]**.** The optical properties of nanomaterials depend on parameters such as feature size, shape, surface characteristics, and other variables including doping and interaction with the surrounding environment or other nanostructures**.** The simplest example is the well-known blue-shift of absorption and photoluminescence spectra of semiconductor nanoparticles with decreasing particle size, particularly when the size is small enough [2]**.**

Zinc oxide (ZnO) is a semiconductor material described by a wide band gap approximately from 3**.**2 to 3**.**3 eV, a high transmission in the range of visible region, a native n-type conductivity as well as by its excellent photoluminescence (PL) properties, which can be modified by the doping of impurities in its structure [1, 3]**.** Thus transition metal-doped ZnO has the potential to be a highly multifunctional material with coexisting magnetic, semiconducting, electromechanical, and optical properties [4]**.** Recently, scientists paid much effort to improve the interfacial charge transfer efficiency and shift the band-gap of ZnO so as to absorb it lightly in the visible region of the solar spectrum**.** The ZnO nanomaterials coupled with other metal oxide semiconductors facilitate enhanced photo-catalytic activity [5]**.**

The subject that currently interests numerous researchers is the enhancement of the optical and electrical properties of ZnO nanostructure by doping with another metals in its structure (Al, Ga, In, Ti, etc**.**). Actually, n-type doping is controlled by the incorporation of certain group elements in the ZnO crystal structure is a repeated method for altering both the bandwidth energy and electrical

*Corresponding author E-mail: emad.badawi@mu.edu.eg

conductivity by increasing the concentration of carriers while keeping high transparency in the range of visible [6]. Most of the previous doped ZnO work is related to doping with group III dopants (Al, Ga, and In), while most recently, new studies have been conducted on quadrivalent dopants like titanium, which can provide two free electrons per atom to improve the conductivity of the ZnO host and to modify the photo-response.

Furthermore, ZnO nanomaterials with a high Ti content have also been researched because of their applications in gas sensors, paint pigments, catalytic sorbents for removal of contaminants from hot coal gases (H_2S, As, etc.), degradation of organic compounds, and photo-catalytic splitting of water, as well as in DSSC, anodes of Li-ion batteries, microwave devices, low-temperature co-fired ceramics, and many more. Also, in comparison with pure ZnO, the composite ZnO/Zinc Titanate has enhanced green emission [7, 8]. The composite ZnO/Zinc Titanate from the ternary nano-composites which intensive efforts have been made to synthesize, which exhibit superior properties that are otherwise impossible by common binary composites. Therefore, the study of ZnO with Ti atoms incorporated and the understanding of the Ti incorporation into the ZnO structure, both as a dopant or in the form of a mixed oxide, is still under debate and constitutes a very interesting challenge. Zinc Titanate ($ZnTiO_3$) has superior electrical properties as reported that are adequate for applications towards microwave dielectrics.

There are three composites that produce in the ZnO –TiO_2 system:$ZnTiO_3$ with a hexagonal ilmenite crystal structure (h-$ZnTiO_3$), Zn_2TiO_4 with a cubic spinel crystal structure, and $Zn_2Ti_3O_8$ with a cubic defect spinel crystal structure [8].

Recently interest in these ZnO-TiO_2 compounds was reactivated because they can combine the characteristics of the individual oxides, ZnO [1, 9, 10] and TiO_2 [11, 12], specially the coupling of ZnO nanoparticles and TiO_2 nanoparticles produced a significant effect on their electronic and physicochemical, photo-electrochemical properties, principally in their surfaces areas and surface morphologies [13]. Moreover, as the recent great scientific and technological interest importance of nanotechnology, nanoparticles in general and those of ZnO-TiO_2 are of due to the special properties they exhibit compared to their micrometric counterpart [14-17]. Because of these novel properties have caused nanoparticles to be find in tremendous amount applications such as catalysts [18, 19], antibacterial [20], drug liberators [21], in electronics, optoelectronics, optical detection, biomedicine and bioimages [14-17]. Meanwhile, Reinosa et al. [22] made a ZnO-TiO_2 composite by taking 15 wt% of TiO_2 nanoparticles mixing with 85 wt% of ZnO microparticles, using a dry nano-dispersion method, a material that obtained a 60% improvement in the Sun Protection Factor (SPF) value when compared with a standard method. Also, this composite by Dynamic light scattering measurements showed that this could be considered as a nano-free UV filter with easy-to-handle characteristics. Newly, Ayed et al. [23] synthesized ZnO-TiO_2 composites by the conventional method of mixing oxides using different weight amounts of TiO_2 (1, 3, 5 and 7 wt%). The obtained mixed powders were annealed at 900 °C for 24 h. The XRD of the sintered samples, showed the presence, of wurtzite type ZnO, as well as spinel-type Zn_2TiO_4 and hexagonal $ZnTiO_3$ compounds. The measurements of optical properties (absorbance and reflectance) carried out by the researchers on these composites showed that the mixing of TiO_2 to ZnO powders favored more transparency in the visible range and two edges of absorption in the UV region [24]. It is possible to obtain a greater photo-catalytic reaction speed and then a greater photo-catalytic activity because electron-hole separation is favored, decreasing the recombination of these charge carriers [25-29]. Also, they have been used for photo-anodes in dye-sensitized solar cells [30], in ink degradation [31-34], herbicide degradation [35], humidity sensors [36-38], and, photo-anodes for water splitting [39, 40] among other applications.

Nano-composites of ZnO-TiO_2 system have been synthesized using varied methods such as chemical vapor deposition [41], sol-gel [42], combustion [43], ultrasonic pyrolysis spray [44], hydrothermal [13], coprecipitation [29], electrospinning [45] thermal decomposition of salts [46], and impregnation [47]. The physicochemical properties of ZnO-TiO_2 nano-composites - and therefore their functionality - as is generally the case with nanoparticles - will be defined by the synthesis method used. As the results from research on other systems show [48], the behavior and functionality of the particle can be significantly affected according to the synthesis method and the history of the processing. To understand and predict the properties of nanoparticles it is thus necessary to guarantee the reliability and reproducibility of the method used to obtain them. The results of Karakoti et al. [48] show that small and apparently insignificant changes can strongly alter the properties of the final product [24].

Sol-gel is considered one of the most popular methods to grow metal oxide nanoparticles (NPs), such as ZnO NPs, because of its simplicity, reliability, reproducibility, and cost effectiveness [49-56]. Meanwhile, citric acid, which is an effective chelating agent, is considered one of the most minor organic molecules commonly used in sol-gel synthesis. In the citric acid sol-gel (citrate route) method, citric acid is mixed with an aqueous metal salt and the prepared solution is heated up to form a viscous solution or Gel. As the "metal-citrate" gel is heated, the organic component burns at ~ 250 – 300 °C. Milling and then annealing the resulting powder produce the metal oxide NPs. During the sol-gel synthesis process, citric acid acts as a chelating agent for metal ions as well as an organic fuel during the calcination process.

Binary, ternary, and quaternary metal oxides can be synthesized by this method in both crystalline and amorphous forms. The main advantage of this method, as

with more traditional sol-gel chemistry, is the homogeneity of the starting material**.** When the 'gels' of the metal–citrate are heated, combustion of the organic component takes place at 300 – 400 °C, depending on the metal counterion and existence of additives**.** The formation of the organic matrix at the first stages of synthesis can ensure that when nucleation take place, the sites are uniformly dispersed and numerous, confirming a small crystallite size**.** The other purpose of the matrix is to ensure that the different metals remain mixed on an atomic scale in the case of ternary or quaternary systems**.**

In the present work, ZnO, and ZnO-TiO_2 nano-composites were synthesized using the citrate route method**.** The synthesized samples were treated at two different temperatures to study and confirm the obtained product doped or the presence of new phases resulting from the interaction of zinc with titanium (Nano-composite)**.** In addition, the obtained powders were characterized to find out their properties, giving special care to the optical properties and establishing a relationship between synthesis-structure properties**.**

2. Experimental details

2.1. Chemicals and Synthesis

As shown in **Fig 1**, Titanium doped ZnO, and nano-composite (TZO samples) were synthesized by the sol-gel method (citrate route method)**.** The materials are used in the synthesis of ZnO nanosheets by the sol-gel method are zinc acetate dehydrate**;** Zn $(AC)_2.2H_2O$ and citric acid (H_3Cit or $C_6H_8O_7$), and titanium isopropoxide (without further purification)**.** Zinc acetate dehydrates; Zn $(AC)_2.2H_2O$ and citric acid (the complexing agent) (H_3Cit or $C_6H_8O_7$) with molar ratio 1**:**2 was dissolved in 25 ml deionized water separately**.** The zinc acetate dehydrates solution was added drop wise into the citric acid solution on a magnetic stirrer at room temperature, after the reaction mixture was maintaining for about an hour at room temperature, a specific amount calculated for %Ti of Titanium isopropoxide was added and kept again for about an hour at room temperature**.** Then the solution was kept at 85 °C on a heated magnetic stirrer, then at 120 °C, until highly viscous residuals were generated, the sample was allowed to dry at 120 °C**.** During continued heating for 1 h at 120, the sol became more and more viscous and finally became a xerogel, which is heated again or burned for 1 h at 250 °C to complete drying, giving brownish-black porous foam. The porous remainder was grounded into a powder then calcined at 400 °C for 1 h to get rid of the carbonaceous materials producing off-white doping or nano-composite product. Similar experiments were repeated with constant M **:** CA molar ratios (i**.**e**.** 1 **:** 2) and varying Ti **:** Zn molar ratios**:** 0**.**008726 **:** 0**.**3998, 0**.**0203 **:** 0**.**3998, 0**.**0312 **:** 0**.**3998, 0**.**0425 **:** 0**.**3998, 0**.**0614 **:** 0**.**3998, 0**.**0795 **:** 0**.**3998, 0**.**0931 **:** 0**.**3998, 0**.**1072 **:** 0**.**3998, and 0**.**1222 **:** 0**.**3998 respectively**.** Then cooled until room temperature was reached and the desired product was obtained**.**

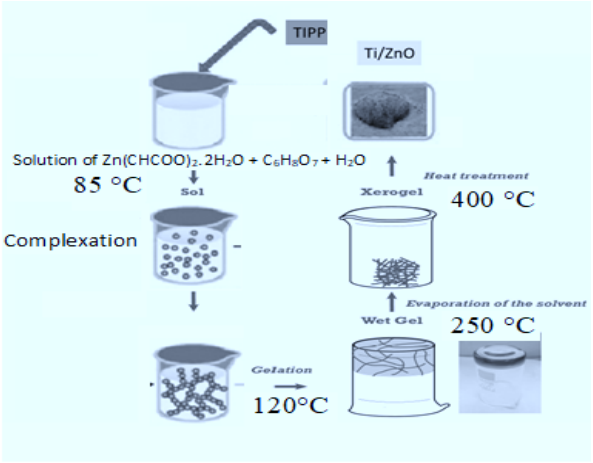

Fig.1 Schematic representation of the synthesis of ZnO – TiO_2 by sol-gel route**.**

2.2. Ultraviolet – Visible (UV – Vis) Spectroscopy

The optical characterization was carried out by measuring the absorbance and the diffuse reflectance spectroscopy in UV-Vis range, which result from the electronic transitions of a solid structure when irradiated with ultraviolet or visible light**.** With the resulting absorption spectrum, it is probable to obtain the value of the width band gap energy [57]**.** The spectra of the prepared powders were obtained with a Shimadzu UV-2600 UV – Vis – spectrophotometer by using the reference material barium sulfate ($BaSO_4$), in the range between 200 and 800 nm, and at 100 nm/min of a scanning speed.

3. Results and discussion

Fig. 2 shows the room temperature UV–vis absorption spectrum of TZO samples prepared with different concentrations of Ti**.**

As seen in **Fig. 2**, first the position of absorption edge (when there is only one absorption edge) around 400 nm is slightly red shifted with increasing the Ti concentration at low Ti content from 2% to 4% M to 6% respectively**.** This red shift may be due to increasing the Ti content on the ZnO nanostructures and change of the band gap**.** Then at high Ti content second absorption edge started to appear and make the change in first edge**.** These absorption edges in the UV region are related to the optical band gap [58], we can see two absorption edges or two reflectance edges**.**

The two absorption peaks: Generally, there is a strong absorption peak of the pure ZnO samples in the range 300 – 400 nm**.** The absorption spectra for the synthesized TZO products, showed strong absorptions at wavelengths 311, and 299 nm associated with $ZnTiO_3$ phase [7], while the absorption peaks located at 373, and 371 nm corresponds to ZnO phase for the samples calcinated at 400, and 600°C respectively**.** There is a blue or red shift after increasing the calcination temperature which may be related**.**

Fig. 3 shows the room temperature UV – vis diffuse reflectance spectra of TZO samples prepared with different concentrations of Ti**.** Similar to the absorbance spectra, shift is observed a round 400 nm that increases with Ti doping**.** Then at high Ti content, a second reflectance edge appears which affects the first edge and the band gap**.**

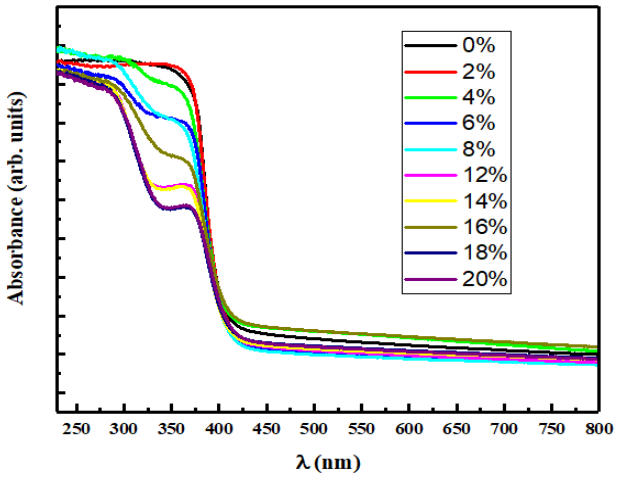

Fig. 2: Absorption spectra of TZO nanostructures synthesized at different Ti content.

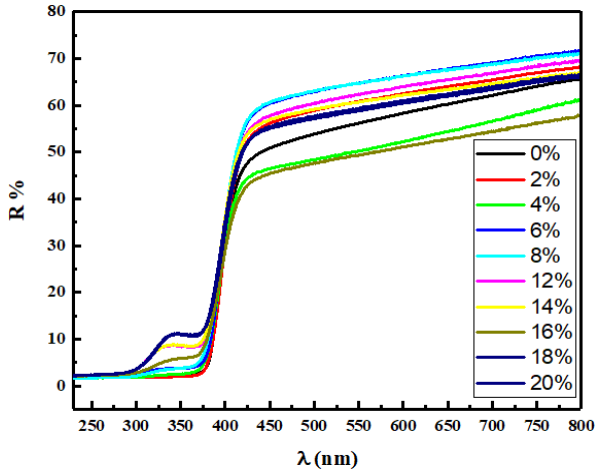

Fig. 3: Diffuse reflectance spectra of TZO nanostructures synthesized at different Ti content.

3.1. The absorption coefficient from UV - vis absorption spectra

Basically absorption coefficient is the measure of light that might be absorbed by a given thickness of a material**.** It tells us how much light corresponding to specific wavelength will be absorbed by a material**.**

$$\alpha = (2.303)\,(A)/L \qquad (1)$$

where, A is the absorbance, and L is the length of the cell**.**

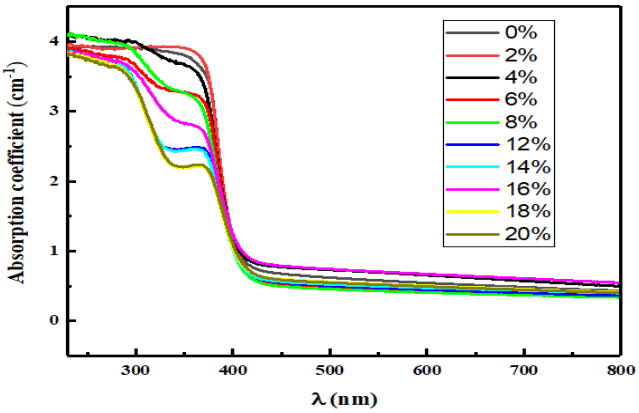

Fig. 4: The Absorption coefficient of TZO nanostructures synthesized at different Ti content.

From this graph **Fig. 4**, the material is showing maximum absorption coefficient nearly at 350 nm**.** So that it can absorb light wavelength at 350 nm more efficiently. The trend of graph showing sharp decrease around 400 nm, then, it going to shifted with increase of Ti content and appearance of another decrease edge**.**

3.2. The extinction coefficient (*K*) from UV-vis absorption spectra

It measures how strongly a chemical species or substance absorb light at particular wavelength**.** It depends on the structure and chemical composition of a substance or material**.** In other words, it is measure of absorption of electromagnetic radiation in medium and lost due to scattering**.**

$$K = \frac{\alpha\lambda}{4\pi} \qquad (2)$$

Where, α is the absorption coefficient and λ is the wavelength**.**

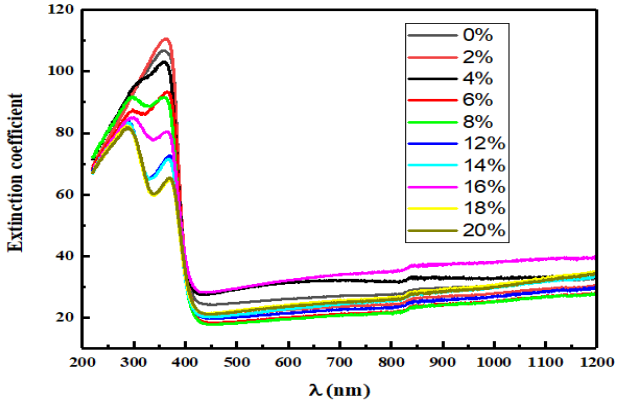

Fig. 5: Extinction coefficient of TZO nanostructures synthesized at different Ti content.

From this graph **Fig. 5**, the extinction coefficient (K) increases with wavelength to a maximum value at 350 nm**.** Then, trend of graph showing sharp decrease around 400 nm then, it going to shifted with increase of Ti content and appearance of another decrease edge**.**

3.3. The refractive index (n) from UV-vis absorption spectra

It is the measurement of how light propagates through a material**.** Higher the refractive index (n), slower will light travel through a material, that changes its direction**.** It is very essential optical constant and play an important role in designing optical devices**.**

$$\boldsymbol{n = \frac{1}{T_s} + \sqrt{\frac{1}{T_s - 1}}} \quad \textbf{(3)}$$

So, T_s is the percent of the transmittance**.**

$$\boldsymbol{T_S = 10^{(-A)} x 100} \quad \textbf{(4)}$$

Where, A is the absorbance**.**

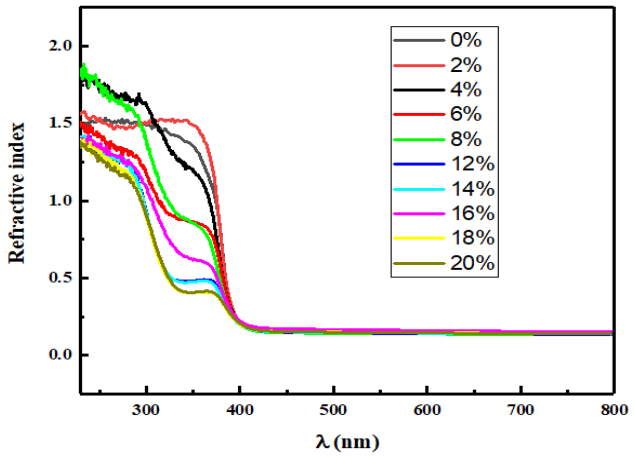

Fig. 6: Refractive index of TZO nanostructures synthesized at different Ti content.

This graph **Fig. 6** shows that, refractive index (n) sharp decreases around at 400 nm, and there is a shift with increasing the Ti content due to the formation of ZnO - $ZnTiO_3$ Nano-composite**.**

3.4. Calculation of Band gap Energy (E_g) from UV-Visible reflectance Spectroscopy

To determine the value of the band gap energy (E_g) of the synthesized samples using the UV-vis diffuse reflectance data, the diffuse reflectance (R) of the sample can be correlated to the Kubelka – Munk Function $F(R)$by the relation [59 - 61]**:**

$$\boldsymbol{F(R) = (1 - R)^2 / 2R} \quad \textbf{(5)}$$

Where R is the reflectance of an infinitely thick layer for which an additional increase in thickness does not change its reflectance**.** This is made for fine powders at only a few millimeters depth**.**

The Kubelka – Munk Function (KMF) is simply expressed as**:**

$$\boldsymbol{F(R) = K/S} \quad \textbf{(6)}$$

where K and S are the absorption and scattering coefficients, respectively**.** Moreover, the KMF and the energy band gap are correlated as**:**

$$\boldsymbol{h\nu\, F(R_\infty)\ \alpha\ (h\nu - E_g)^n} \quad \textbf{(7)}$$

The four values of (n) coincides with the allowed and forbidden transitions mentioned in ref [60]**.** Finally, the energy gap (E_g), supposing allowed direct transition, can be found from a graph of $[h\nu\, F(R_\infty)]^2$ plotted versus $h\nu$**.** This graph is represented in **Fig. 7.** The extrapolated linear portion of the graph intersection the $h\nu$ - axis gives the optical energy band, which can be assuming allowed indirect as in ref [62]**.**

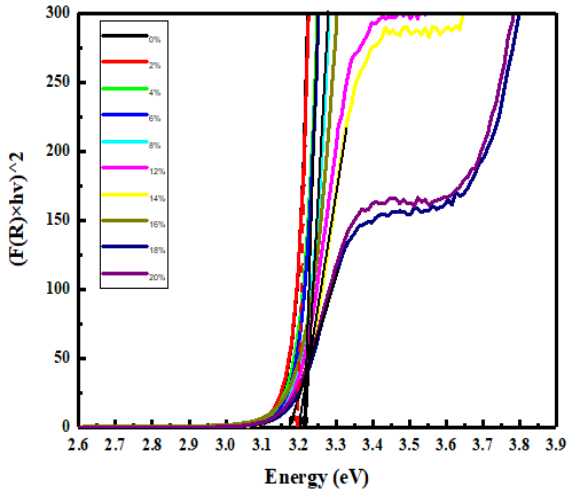

Fig. 7: Tauc plot by UV-vis reflectance data used for extracting the band gap.

3.5. Calculation of Bandgap Energy (E_g) from UV-Visible Absorption Spectroscopy

The band-gap energy (E_g) values of the TZO samples were calculated by applying the absorption band-edge of the corresponding samples using *Tauc's* plot [63]**.**

$$\boldsymbol{(\alpha h\nu)^n = k\,(h\nu - E_g)} \quad \textbf{(8)}$$

Where α is the absorption coefficient, E_g is the band-gap energy and k is the absorption constant**.** The absorption coefficient (α) was determined from the equation (1)**.**

The optical band gap energy (E_g) of nanostructures can be estimated by using the last equation of UV-visible

absorption data. In this relation, "α" is the absorption coefficient, "$h\nu$" is the energy of the incident photon, "k" is the energy independent constant and E_g is the optical band gap energy of the material. In this relation the exponent "n" denotes the nature of transition. For direct band gap material $n = 2$, while for indirect $n = ½$.

From the plotting **Fig. 8** between $(\alpha h\nu)^n$ and $h\nu$ (energy of the incident photon) which has a linear relationship then E_g (the band gap energy) is obtained by extrapolating the straight-line portion of the plot to zero absorption coefficient. A single slope in the plot explain the direct and allowed transition. The band gap energy increases slightly with increasing the Ti% and then decreases at higher Ti content as shown in **Table 1.**

This result shows that the band gap energy of the TZO nano-composite system can be tuned by varying the Ti% for different applications. As shown in **Table 1**, the band gap was tuned from 3.16 to 3.07 eV by raising the Ti content.

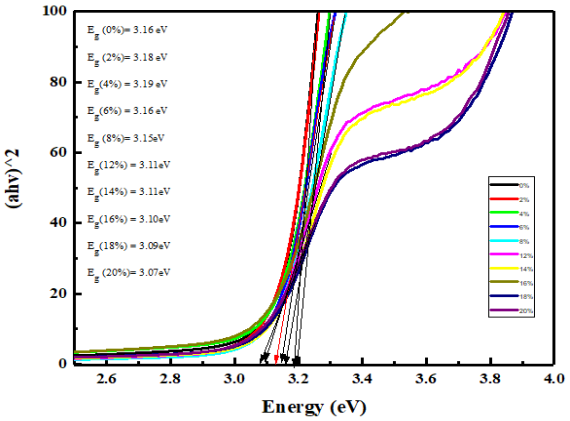

Fig. 8: Tauc plot by UV-vis absorption data used for extracting the band gap.

Table 1: The energy band gap of TZO nanostructures synthesized at different Ti content from Kubelka-Munk plot and from Tauck plot.

Ti%	Kubelka		Tauck	
0	Eg (0%) = 3.18 eV	Undoped	Eg (0%) = 3.16 eV	Undoped
2	Eg (2%) = 3.19 eV	Increase doped	Eg (2%) = 3.18 eV	Increase doped
4	Eg (4%) = 3.20 eV	Increase doped	Eg (4%) = 3.19 eV	Increase doped
6	Eg (6%) = 3.20 eV	Doped or composite	Eg (6%) = 3.16 eV	Doped or composite
8	Eg (8%) = 3.20 eV	Doped or composite	Eg (8%) = 3.15 eV	Doped or composite
12	Eg (12%) = 3.18 eV	Decrease composite	Eg (12%) = 3.11 eV	Decrease composite
14	Eg (14%) = 3.18 eV	Decrease composite	Eg (14%) = 3.11 eV	Decrease composite
16	Eg (16%) = 3.18 eV	Decrease composite	Eg (16%) = 3.10 eV	Decrease composite
18	Eg (18%) = 3.16 eV	Decrease composite	Eg (18%) = 3.09 eV	Decrease composite
20	Eg (20%) = 3.16 eV	Decrease composite	Eg (20%) = 3.07 eV	Decrease composite

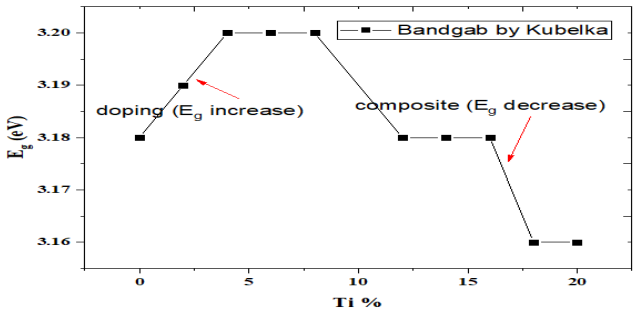

(a)

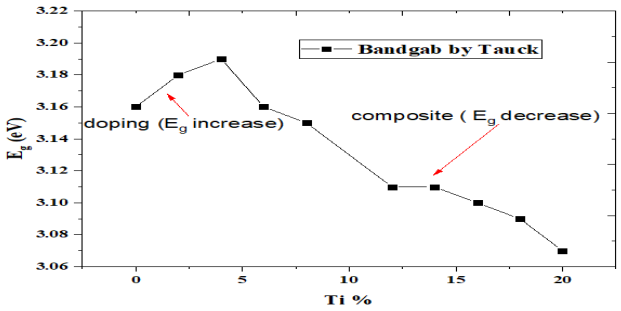

(b)

Fig. 9: The energy band gap of TZO nanostructures synthesized at different Ti content from (a) Kubelka-Munk plot and (b) from Tauck plot.

The calculated band gaps of TZO samples were found as shown in **Fig. 9.** The results confinement with the results reported in refs. [5, 64, 65]. Where the change in the band gap can be explained by the change in particle size, change of structure, and doping.

The intercepts gives the direct energy band gaps for the 0%, 2%, 4%, 18%, and 20% samples are in **Table 1**, the band gap was found to be 3.16 eV. From the reflectance above data two features are significantly evident: First, a slight blue-shift in the energy band gap of 0.04 eV for TZO samples up to 8% low Ti-doped is observed as compared to the undoped ZnO. This blue-shift might be explained by the effect of Ti

doping at the Zn sites in ZnO crystal structure resulting in the change in energy band gap**.** Since, Ti atoms when substituted at Zn site in ZnO lattice acts as a donor atom by supplying two free electrons, the increase in the optical band gap with electron concentration the so called Burstein – Moss BM band filling effect [65] which is due to the filling of lower states in the conduction band**.** Chung et al**.** also detected a blue-shift in energy band gap in Ti doped ZnO films**.** This feature in the excitonic band is mostly responsible for the characteristics of quantum confinement effects. In the quantum confinement range where the band gap of the particle increases causing the shift in absorption edge to lower wavelength, as the particle size decreases**.** Second, for a higher Ti% in the samples, the nano-composite produce (two phases), the wurtzite-like structure increasingly becomes more amorphous (w-ZnO + mixed oxides, associated with $ZnTiO_3$ phase) the band gap energy becomes red shifted further within TZO samples from 3**.**19 to 3**.**10 eV with the Ti% further increase as mentioned in [66]**.** Finally, in a highly doped sample (Ti% = 18%, and 20%) the band gap decreases to 3**.**10 eV**.** In this case, this value cannot be explained by the doping effect, but instead, it could have been caused by the presence of a different amorphous TZO compound (mixed oxides) in the visible range which gives very important applications**.**

3.6. Calculation of the particle size from UV – vis spectra

The Average particle size (r) of the nano material was calculated using the following equation for effective mass approximation (**Eq. 9**)**.** This equation describes the particle size in radius as a function of peak absorbance wave length for Ti doped ZnO**.**

$$r(nm) = \left[\left\{\frac{-0.2963 + (-40.1970 + \frac{13620}{\lambda_p})}{-7.34 + \frac{2418.6}{\lambda_p}}\right\}\right]^2 \qquad (9)$$

From the above relation, the particle size (r) was found as shown in Table 2**.**

Table 2: Average particle size (r) determined using UV-vis spectra

Sample	Average particle size using UV-vis spectra (nm)
0%	22.9972924
2%	22.91498679
4%	23.73599942
6%	23.73599942
8%	25.72466447
12%	23.99044639
14%	23.99044639
16%	25.91964445
18%	24.22924396
20%	24.22924396

From this table, it is clear that the size (r) ranged from 22 to 25 nm**.**

4. Conclusions

We have demonstrated that Zinc oxide (ZnO) and TZO samples having different Ti content can be synthesized from doping to composite by Citrate sol-gel method**.** The results show the band gap energy of Ti- doped ZnO to increase from 3**.**16 to 3**.**20 achieve a red shift (increase the absorbance by decreasing the energy gab) and a blue shift from 3**.**19 to 3**.**07 eV (decrease the absorbance by increasing the energy gab) in the visible range which has a very important application, this improves the optical properties of the ZnO and gives an indication on how to tune its band gab (increase or decrease by doping or composition)**.** This result shows that the band gap energy of the TZO ($ZnO/ZnTiO_3$) nano-composites system can be tuned by varying the Ti content for different applications**.** On the other hand, it is clear that the average particle size (r) ranged from 22 to 25 nm**.**

References

[1] Ü**.** Özgür, Y**.** I**.** Alivov, C**.** Liu, A**.** Teke, M**.** Reshchikov, S**.** Doğan, V. Avrutin, S.-J. Cho, and H. Morkoçd, A comprehensive review of ZnO materials and devices, *Journal of applied physics.* , **98**, 1-103, (2005)**.**

[2] J**.** Z**.** Zhang, *Optical properties and spectroscopy of nanomaterials***,** World Scientific,UK,18-24, (2009)**.**

[3] P**.** A**.** Rodnyi and I**.** V**.** Khodyuk, Optical and luminescence properties of zinc oxide (Review), *Optics and Spectroscopy,* **111**, 776-785 (2011)**.**

[4] R**.** Janisch, P**.** Gopal, and N**.** A**.** Spaldin, Transition metal-doped TiO_2 and ZnO –present status of the field, *Journal of Physics: Condensed Matter,***17**, 657- 689 (2005)**.**

[5] R**.** Dhanalakshmi, A**.** Pandikumar, K**.** Sujatha, and P**.** Gunasekaran, Photocatalytic and antimicrobial activities of functionalized silicate sol – gel embedded ZnO – TiO ₂ nanocomposite materials, *Materials Express,***3**, 291-300 (2013)**.**

[6] L**.** Irimpan, B**.** Krishnan, V**.** P**.** Nampoori, and P**.** Radhakrishnan, Luminescence tuning and enhanced nonlinear optical properties of nanocomposites of ZnO -TiO_2, *J Colloid Interface Sci,***324**, 99-104 (2008)**.**

[7] M**.** Jose, M**.** Elakiya, and S**.** A**.** M**.** B**.** Dhas, Structural and optical properties of nanosized

ZnO/ZnTiO3 composite materials synthesized by a facile hydrothermal technique, *Journal of Materials Science: Materials in Electronics,* **28**, 13649-13658 (2017).

[8] Y. C. Lee, Y. L. Huang, W. H. Lee, and F. S. Shieu, Formation and transformation of $ZnTiO_3$ prepared by sputtering process, *Thin Solid Films,* **518**, 7366-7371(2010).

[9] C. Klingshirn, ZnO material, physics and applications, *PhysChem,* 8, 782-803 (2007).

[10] A. Moezzi, A. M. McDonagh, and M. B. Cortie, Zinc oxide particles: Synthesis, properties and applications, *Chemical Engineering Journal,* **185-186**, 1 -22 (2012).

[11] X. Chen and S. S. Mao, Titanium Dioxide Nanomaterials: Synthesis, Properties, Modifications, and Applications, *Chemical Reviews,* **107**, 2891-2959 (2007).

[12] S. M. Gupta and M. Tripathi, A review of TiO_2 nanoparticles, *Chinese Science Bulletin,* **56**, 1639-1657 (2011).

[13] D. Chen, H. Zhang, S. Hu, and J. Li, Preparation and Enhanced Photoelectrochemical Performance of Coupled Bicomponent ZnO − TiO_2 Nanocomposites, *The Journal of Physical Chemistry C,* **112**, 117-122 (2008).

[14] K. J. Klabunde and R. M. Richards, *Nanoscale materials in chemistry*: John Wiley & Sons, Hoboken, New Jersey 539-579 (2009).

[15] D. S. English, Book Review of Inorganic Nanoparticles: Synthesis, Applications, and Perspectives, *Journal of the American Chemical Society,* **133**, 9626-9626 (2011).

[16] K. Lu, *Nanoparticulate materials: synthesis, characterization, and processing*: John Wiley & Sons, Hoboken, New Jersey, 128-189 (2013).

[17] F. Bensebaa, "Nanoparticle Technology: from Lab to Market," ed: Elsevier Ltd., Amsterdam, 2012.

[18] M. B. Gawande, A. Goswami, F.-X. Felpin, T. Asefa, X. Huang, R. Silva, *et al.*, "Cu and Cu-based nanoparticles: synthesis and applications in catalysis, *Chemical reviews,* **116**, 3722-3811(2016).

[19] H. Abe, J. Liu, and K. Ariga, "Catalytic nanoarchitectonics for environmentally compatible energy generation," *Materials Today,* **19**,12-18, (2016).

[20] S. Stankic, S. Suman, F. Haque, and J. Vidic, "Pure and multi metal oxide nanoparticles: synthesis, antibacterial and cytotoxic properties," *Journal of Nanobiotechnology,* **14:73**,1-20 (2016).

[21] W. Park and K. Na, "Advances in the synthesis and application of nanoparticles for drug delivery," *Wiley Interdisciplinary Reviews: Nanomedicine and Nanobiotechnology,* **7**, 494-508 (2015).

[22] J. Jiménez Reinosa, P. Leret, C. M. Álvarez-Docio, A. del Campo, and J. F. Fernández, "Enhancement of UV absorption behavior in ZnO – TiO_2 composites," *Boletín de la Sociedad Española de Cerámica y Vidrio,* **55**,55-62 (2016).

[23] S. Ayed, R. Ben Belgacem, J. O. Zayani, and A. Matoussi, "Structural and optical properties of ZnO/TiO2 composites," *Superlattices and Microstructures,* **91**, 118-128 (2016).

[24] A. Mazabuel-Collazos, C. D. Gómez, and J. E. Rodríguez-Páez, "ZnO - TiO_2 nanocomposites synthesized by wet-chemical route: Study of their structural and optical properties," *Materials Chemistry and Physics,* **222**, 230-245(2019).

[25] S. S. Silva, F. Magalhães, and M. T. C. Sansiviero, "Nanocompósitos semicondutores ZnO/TiO_2: testes fotocatalíticos," *Química nova,* **33**,85-89 (2010).

[26] G. Marcì, V. Augugliaro, M. J. López-Muñoz, C. Martín, L. Palmisano, V. Rives, *et al.*, "Preparation Characterization and Photocatalytic Activity of Polycrystalline ZnO/TiO_2 Systems. 1. Surface and Bulk Characterization," *The Journal of Physical Chemistry B,* **105**,1026-1032 (2001).

[27] G. Marcì, V. Augugliaro, M. J. López-Muñoz, C. Martín, L. Palmisano, V. Rives, *et al.*, "Preparation Characterization and Photocatalytic Activity of Polycrystalline ZnO/TiO_2 Systems. 2. Surface, Bulk Characterization, and 4-Nitrophenol Photodegradation in Liquid−Solid Regime," *The Journal of Physical Chemistry B,* vol. **105**,1033-1040 (2001).

[28] C. Cheng, A. Amini, C. Zhu, Z. Xu, H. Song, and N. Wang, "Enhanced photocatalytic performance of TiO_2-ZnO hybrid nanostructures," *Scientific Reports,* **4**, 1-5 (2014).

[29] V. Lachom, P. Poolcharuansin, and P. Laokul, "Preparation, characterizations and photocatalytic activity of a ZnO/TiO_2 nanocomposite," *Materials Research Express,* **4 (3)** 11-19(2017).

[30] K. P. Shejale, D. Laishram, R. Gupta, and R. K. Sharma, "Zinc Oxide – Titania Heterojunction-based Solid Nanospheres as Photoanodes for Electron-Trapping in Dye-Sensitized Solar Cells," *Energy Technology,* **5**,489-494 (2017).

[31] J. Chen, W. Liao, Y. Jiang, D. Yu, M. Zou, H. Zhu, *et al.*, "Facile Fabrication of ZnO/TiO_2 Heterogeneous Nanofibres and Their Photocatalytic Behaviour and Mechanism towards Rhodamine B," *Nanomaterials and Nanotechnology,* **6**, 1-8 (2016).

[32] M. Konyar, D. Ovali, H. C. Yatmaz, C. Duran, and K. Öztürk, "Photocatalytic efficiency of ZnO/TiO_2 composite plates in degradation of RR180 dye solutions," *Advances in Science and Technology*, **65**, 244-250 (2010).

[33] J. Guo, J. Li, A. Yin, K. Fan, and W. Dai, "Photodegradation of Rhodamine B on Sulfur Doped ZnO/TiO_2 Nanocomposite Photocatalyst

under Visible-light Irradiation," *Chinese Journal of Chemistry,***28**, 2144-2150 (2010).

[34] H. Bel Hadjltaief, M. Ben Zina, M. E. Galvez, and P. Da Costa, "Photocatalytic degradation of methyl green dye in aqueous solution over natural clay-supported ZnO – TiO_2 catalysts," *Journal of Photochemistry and Photobiology A: Chemistry,***315**, 25-33 (2016).

[35] M. Gholami, M. Shirzad-Siboni, M. Farzadkia, and J. K. Yang, "Synthesis, characterization, and application of ZnO/TiO_2 nanocomposite for photocatalysis of a herbicide (Bentazon)," *Desalination and water treatment,***57**,13632-13644 (2016).

[36] B. C. Yadav, R. Srivastava, and C. D. Dwivedi, "Synthesis and characterization of ZnO – TiO_2 nanocomposite and its application as a humidity sensor," *Philosophical Magazine,***88**,1113-1124 (2008).

[37] L. Gu, K. Zheng, Y. Zhou, J. Li, X. Mo, G. R. Patzke*, et al.*, "Humidity sensors based on ZnO/TiO_2 core/shell nanorod arrays with enhanced sensitivity," *Sensors and Actuators B: Chemical,* **159**, 1-7(2011).

[38] N. K. Pandey, K. Tiwari, and A. Roy, "ZnO – TiO_2 nanocomposite: Characterization and moisture sensing studies," *Bulletin of Materials Science,***35**, 347-352(2012).

[39] K. Pan, Y. Dong, W. Zhou, Q. Pan, Y. Xie, T. Xie*, et al.*, "Facile Fabrication of Hierarchical TiO_2 Nanobelt/ZnO Nanorod Heterogeneous Nanostructure: An Efficient Photoanode for Water Splitting," *ACS Applied Materials & Interfaces,***5**, 8314-8320 (2013).

[40] S. Hernández, V. Cauda, A. Chiodoni, S. Dallorto, A. Sacco, D. Hidalgo*, et al.*, "Optimization of 1D ZnO@TiO_2 Core–Shell Nanostructures for Enhanced Photoelectrochemical Water Splitting under Solar Light Illumination," *ACS Applied Materials & Interfaces,***6**,12153-12167 (2014).

[41] D. Barreca, E. Comini, A. P. Ferrucci, A. Gasparotto, C. Maccato, C. Maragno*, et al.*, "First example of ZnO − TiO_2 nanocomposites by chemical vapor deposition: structure, morphology, composition, and gas sensing performances," *Chemistry of Materials,***19**,5642-5649 (2007).

[42] Y. Dimitriev, Y. Ivanova, A. Staneva, L. Alexandrov, M. Mancheva, R. Yordanova*, et al.*, "SYNTHESIS OF SUBMICRON POWDERS," *Journal of the University of Chemical Technology and Metallurgy,***44**,235-242 (2009).

[43] A. Bachvarova-Nedelcheva, R. Iordanova, A. Stoyanova, R. Gegova, Y. Dimitriev, and A. Loukanov, "Photocatalytic properties of ZnO/TiO_2 powders obtained via combustion gel method," *Open Chemistry,***11**,364-370 (2013).

[44] K. Ohshima, K. Tsuto, K. Okuyama, and N. Tohge, "Preparation of ZnO - TiO_2 Composite Fine Particles Using the Ultrasonic Spray Pyrolysis Method and Their Characteristics on Ultraviolet Cutoff," *Aerosol Science and Technology,***19**, 468-477 (1993).

[45] X. Liu, Y.-y. Hu, R.-Y. Chen, Z. Chen, and H.-C. Han, "Coaxial Nanofibers of ZnO-TiO_2 Heterojunction With High Photocatalytic Activity by Electrospinning Technique," *Synthesis and Reactivity in Inorganic, Metal-Organic, and Nano-Metal Chemistry ,***44**, 449-453(2014).

[46] M. A. Habib, M. T. Shahadat, N. M. Bahadur, I. M. I. Ismail, and A. J. Mahmood, "Synthesis and characterization of ZnO-TiO_2 nanocomposites and their application as photocatalysts," *International Nano Letters,***3(5)**, 1-8 (2013).

[47] W. Ahmad, U. Mehmood, A. Al-Ahmed, F. A. Al-Sulaiman, M. Z. Aslam, M. S. Kamal*, et al.*, "Synthesis of zinc oxide/titanium dioxide (ZnO/TiO_2) nanocomposites by wet incipient wetness impregnation method and preparation of ZnO/TiO_2 paste using poly(vinylpyrrolidone) for efficient dye-sensitized solar cells," *Electrochimica Acta,***222**,473-480 (2016).

[48] A. S. Karakoti, P. Munusamy, K. Hostetler, V. Kodali, S. Kuchibhatla, G. Orr*, et al.*, "Preparation and characterization challenges to understanding environmental and biological impacts of ceria nanoparticles," *Surface and Interface Analysis,***44**, 882-889(2012).

[49] M. S. Ghamsari, M. R. Gaeeni, W Han, and Hyung-H. Park, *Materials Express*,**7(1)**, 72-78 (2017).

[50] S.S.Alias,A.B.Ismail and A.A.Mohamad*, J. Alloys and Compounds*, **499**, 231-237 (2010).

[51] C. A. J. Eixenberger, K. Wada, K. Reddy, R. Brown, J. Moreno-Ramirez, A. Weltner, C. Karthik, D. Tenne, D. Fologea, D. Wingett, Defect Engineering of ZnO Nanoparticles for Bio-imaging Applications *ACS Appl. Mater. Interfaces*, **11**, 24933-24944 (2019)

[52] A. K. Zak, M. E. Abrishami,W Abd. Majid, R. Yousefi, S. Hosseini, Effects of annealing temperature on some structural and optical properties of ZnO nanoparticles prepared by a modified sol–gel combustion method *Ceramic. International*, **37(1)**, 393-398 (2011) .

[53] K.Omri, I. Najeh,R.Dhahri, J.El Ghoul.L. El Mir, Effects of temperature on the optical and electrical properties of ZnO nanoparticles synthesized by sol–gel method, *Microelectron. Engineering*,**128**, 53-58 (2014).

[54] M. S. M. Ciciliati, D. Fernandes, M. de Melo, A. Hechenleitner, E. Pineda, Fe-doped ZnO nanoparticles: Synthesis by a modified sol–gel method and characterization, Materils. Letters, **159** ,84-86 (2015).

[55] S. Dutta,S. Sarkar and B. N. Ganguly, J. Materils . Sciences and Engineering , **3(1)** ,1-8 (2014).

[56] R. M. Alwan, Q. A. Kadhim, K. M. Sahan, R. A. Ali, R. J. Mahdi, N. A. Kassim, A. N. Jassim, *Nanoscience and Nanotechnology*, **5(1),** 1-6 (2015) .

[57] R. López and R. Gómez, "Band-gap energy estimation from diffuse reflectance measurements on sol–gel and commercial TiO_2**:** a comparative study," *Journal of Sol-Gel Science and Technology,***61**, 1-7 (2012.

[58] M. J. Pawar, V. B. Nimbalkar, Synthesis and phenol degradation activity of Zn and Cr doped TiO_2 Nanoparticles. *Research Journal of Chemical Sciences,* **2(1)**, 32-37 (2012).

[59] A. Mazabuel-Collazos, C. D. Gómez, and J. Rodríguez-Páez, "ZnO-TiO_2 nanocomposites synthesized by wet-chemical route: Study of their structural and optical properties," *Materials Chemistry and Physics,***222**, 230-245 (2019).

[60] R. López and R. Gómez, "Band-gap energy estimation from diffuse reflectance measurements on sol–gel and commercial TiO_2: a comparative study," *Journal of sol-gel science and technology, .* **61**, 1-7(2012).

[61] A. Escobedo-Morales, I. Ruiz-López, M. d. Ruiz-Peralta, L. Tepech-Carrillo, M. Sánchez-Cantú, and J. Moreno-Orea, "Automated method for the determination of the band gap energy of pure and mixed powder samples using diffuse reflectance spectroscopy," *Heliyon,* **5(4)**, 1-19 (2019).

[62] S. Perween and A. Ranjan, "Improved visible-light photocatalytic activity in $ZnTiO_3$ nanopowder prepared by sol-electrospinning," *Solar Energy Materials and Solar Cells,***163**, 148-156 (2017).

[63] T. Suprabha, H. G. Roy, J. Thomas, K. P. Kumar, and S. Mathew, "Microwave-assisted synthesis of titania nanocubes, nanospheres and nanorods for photocatalytic dye degradation," *Nanoscale research letters,* **4**, 144-152 (2009).

[64] Z. Y.Ye, H. L. Lu,Y. Geng , Y. Z. Gu,Z. Y. Xie, Y. Zhang, and D. W.Zhang, Structural, electrical, and optical properties of Ti-doped ZnO films fabricated by atomic layer deposition. Nanoscale research letters, **8(1)**, 1-6 (2013).

[65] M. Yuste, R. Escobar-Galindo, N. Benito, C. Palacio, O. Martínez, J. Albella*, et al.*, Effect of the Incorporation of Titanium on the Optical Properties of ZnO Thin Films: From Doping to Mixed Oxide Formation *Coatings,* **9(3)**, 1-12 (2019).

[66] S. Perween, A. Ranjan, Improved visible-light photocatalytic activity in $ZnTiO_3$ nano powder prepared by sol-electrospinning. *Solar Energy Materials and Solar Cells*, **163**, 148-156 (2017).